ChemPubSoc Europe

FULL PAPERS

FERM conclusions: A novel lead compound for inhibition of the antibacterial drug target, glutamate racemase, was optimized for both potency and lipophilic efficiency. A hybrid MD–docking and scoring scheme, FERM-SMD, was used to predict the relative potencies of potential derivatives prior to chemical synthesis.

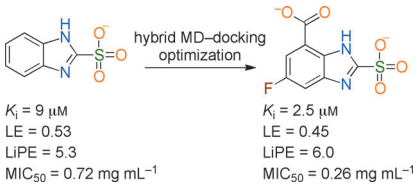

*K. L. Whalen, A. C. Chau, M. A. Spies**

■■ – ■■

In silico Optimization of a Fragment-Based Hit Yields Biologically Active, High-Efficiency Inhibitors for Glutamate Racemase

DOI: 10.1002/cmdc.201300271

In silico Optimization of a Fragment-Based Hit Yields Biologically Active, High-Efficiency Inhibitors for Glutamate Racemase

Katie L. Whalen,[a, b] Anthony C. Chau,[b] and M. Ashley Spies*[a]

A novel lead compound for inhibition of the antibacterial drug target, glutamate racemase (GR), was optimized for both ligand efficiency and lipophilic efficiency. A previously developed hybrid molecular dynamics–docking and scoring scheme, FERM-SMD, was used to predict relative potencies of potential derivatives prior to chemical synthesis. This scheme was successful in distinguishing between high- and low-affinity binders with minimal experimental structural information, saving time and resources in the process. In vitro potency was increased approximately fourfold against GR from the model organism, *B. subtilis*. Lead derivatives show two- to fourfold increased antimicrobial potency over the parent scaffold. In addition, specificity toward *B. subtilis* over *E. coli* and *S. aureus* depends on the substituent added to the parent scaffold. Finally, insight was gained into the capacity for these compounds to reach the target enzyme in vivo using a bacterial cell wall lysis assay. The outcome of this study is a novel small-molecule inhibitor of GR with the following characteristics: $K_i = 2.5\ \mu M$, $LE = 0.45\ kcal\,mol^{-1}\,atom^{-1}$, $LiPE = 6.0$, $MIC_{50} = 260\ \mu g\,mL^{-1}$ against *B. subtilis*, $EC_{50,lysis} = 520\ \mu g\,mL^{-1}$ against *B. subtilis*.

Introduction

In an era of increasingly prolific multi- and total-drug resistant species of bacteria such as *E. coli*, *M. tuberculosis*, and *S. aureus*, the need for rapid discovery of novel antibiotic classes is greater than ever. Compounding this problem is the pronounced dearth of both antimicrobial lead compounds and USFDA-approved drugs emerging from the drug discovery enterprise, including both academia and industry.[1] An illuminating review by O'Shea and Moser[2] reveals that no novel class of antibacterials was developed and approved between 1960 and 2001, despite exhaustive efforts and the parallel development of key techniques. Since the introduction of streptogramins and quinolones in the early 1960s, the growing need for antimicrobials has outpaced the rate of approval of novel drugs. Passage down the pipeline of drug discovery is complicated by the requirement that any antimicrobial target must be essential within a class of bacteria as well as non-essential or absent in humans, or must possess significant structural distinction from any human homologues. Additionally, inhibitors must satisfy stringent physicochemical requirements that ensure bioavailability, minimal toxicity, and efficacy. Recent reviews of the current state of affairs in drug discovery reveal that the lack of chemical diversity in high-throughput screening (HTS)- and genomics-based drug discovery campaigns has been a significant culprit in the failure to obtain novel antimicrobial lead compounds.[1,3]

Bacteria require a number of D-amino acids for biosynthesis of the peptidoglycan cell wall. It has been well established that improper peptidoglycan cross-linking is the basis for a number of known antimicrobial drugs, including the β-lactam class and vancomycins, which act to promote osmotic lysis.[4] In addition to the prevention of peptidoglycan cross-linking directly, the inhibition of enzymes that catalyze the formation of D-amino acids also leads to lysis through accumulation of high internal osmotic pressure. The two ubiquitous D-amino acids in bacterial cell walls are D-alanine and D-glutamate, which are biosynthesized by alanine and glutamate racemases, respectively. The natural product D-cycloserine is a mechanism-based inhibitor of alanine racemase (AR), a PLP-containing enzyme, and has been shown to kill bacteria by making them osmotically sensitive.[5] Similar studies have also been carried out on glutamate racemase (GR, EC 5.1.1.3) inhibitors, establishing a mode of action that involves compromised maturation of the peptidoglycan cell wall.[6] Unlike AR, GR is a cofactor-independent racemase, which catalyzes a stepwise proton abstraction/donation via two cysteine residues acting in a general acid/base mechanism.[7] The general α/β-fold forms two domains, which enclose a relatively small buried active site that is saturated with polar residues. Not surprisingly, GR knockout studies on several pathogenic organisms resulted in D-glutamate auxotrophs.[8] Thus, the strategy of attenuating the pool of D-amino acids is an attractive option for the development of novel antimicrobial agents. However, the only compound in this class that is approved for clinical use is the natural product D-cycloserine, and

[a] K. L. Whalen, Dr. M. A. Spies
Division of Medicinal and Natural Products Chemistry
Department of Biochemistry, University of Iowa
115 South Grand Avenue, Iowa City, IA 52242 (USA)
E-mail: michael-spies@uiowa.edu

[b] K. L. Whalen, A. C. Chau
Department of Biochemistry
University of Illinois at Urbana-Champaign
600 South Mathews Avenue, Urbana, IL 61801 (USA)

Supporting information for this article is available on the WWW under http://dx.doi.org/10.1002/cmdc.201300271.

only in combination with other antibiotics, owing to its undesirable side effects.

To date, only a handful of potent inhibitors have been discovered for bacterial GRs. A structure–activity relationship (SAR) approach produced a 4S-substituted D-glutamate analogue with low-micromolar potency against GR from *S. pneumoniae*, but which suffered from species specificity due to steric clash with a species-variable valine bridge to a hydrophobic pocket proximal to the binding cleft.[9] Later, an HTS campaign of nearly 400 000 compounds resulted in the serendipitous discovery of an uncompetitive inhibitor that binds to a species-specific allosteric site.[6] More recently, a virtual screening campaign targeting a transition-state-like model of the target enzyme produced several low-micromolar competitive inhibitors.[10] A clear trend in the molecular makeup of these inhibitors emerged: aromatic or cyclic compounds containing sulfonic acid moieties. This is not surprising considering previous work that supports the presence of a cyclic carbanion/dienolate transition in the glutamate racemase reaction, which places significant negative charge density at the back of the active site.[11] The superiority of these sulfonic acids over carboxylates (such as that in the natural substrate) could be due to the more dispersed partial negative charge in the sulfonate relative to the sp^2 hybridization of a carboxylate. Most recently, a unique ensemble docking scheme was applied to GR from *B. subtilis* to successfully rank several sulfonate-containing aromatic compounds with potencies ranging from low micromolar to high millimolar.[12] The best of these compounds, 1*H*-benzimidazole-2-sulfonic acid ($K_i = 9$ μM) is the subject of this study.

Herein we present a fragment-based approach to optimization of the previously mentioned lead compound using entirely in silico methods for derivative ranking prior to synthesis and experimental testing. Fragment-based methods offer a number of distinct advantages in drug discovery, particularly optimization of ligand efficiency (LE) and lipophilic efficiency (LiPE) while maintaining potency.[13] Placement and subsequent scoring of potential derivative compounds was achieved via ensemble docking with a unique scoring scheme described by Whalen and co-workers.[12] In the current study, 33 derivatives of the lead compound were docked to an ensemble of conformations generated by using steered molecular dynamics (MD) and ranked using a modified binding energy score. Six derivatives were synthesized and assayed experimentally, resulting in the discovery of two competitive inhibitors with increased inhibitory potency, as well as excellent ligand and lipophilic efficiencies. Compounds were also assayed for bacterial growth inhibition as well as induction of cell wall lysis, ultimately establishing that this class of GR inhibitors targets bacterial cell wall synthesis in vivo.

Results and Discussion

BISA, a scaffold for optimization

Compound **1** (4-hydroxy-1,3-benzenedisulfonic acid, see Figure 4 below) was discovered in a virtual screening campaign against GR using the Chemical Computing Group lead-like library (~1 million compounds).[10] The inhibitory constant against GR from *B. subtilis* was 58 ± 13 μM. Scaffold hopping to compound **2** (1*H*-benzimidazole-2-sulfonic acid, Figure 4 below) increases affinity against this target to a K_i value of 9 ± 2 μM. Compound **2** also shows equal potency against two isozymes of GR from *B. anthracis* (RacE1 and RacE2) as well as GR from *F. tularensis* (MurI), two bacterial species currently considered as Tier 1 Biological Select Agents by the US Government (Figure 1). The high LE of this fragment, coupled with its cross-species activity made compound **2** an ideal candidate for optimization.

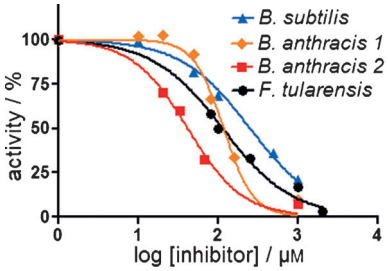

species	IC_{50} / μM
B. subtilis	250 ± 20
B. anthracis 1	120 ± 5
B. anthracis 2	40 ± 5
F. tularensis	110 ± 12

Figure 1. IC_{50} curves for the parent compound **2** against a range of GR isozymes isolated from the indicated bacterial species. IC_{50} values were acquired by fitting to a dose–response curve and represent the mean ± standard error for the nonlinear regression of a single, representative curve.

To generate a basis for rational lead optimization, a basic understanding of the physicochemical components of binding between ligand and receptor is required. As an alternative to X-ray crystallography or NMR spectroscopy, virtual docking was used to generate structural information regarding the interaction of GR and compound **2**. Compound **2** was docked into GR in silico by using a previously solved crystal structure (PDB ID: 1ZUW) as the receptor. The result of docking shows compound **2** with its sulfonic acid moiety situated in the most buried region of the active site, between the catalytic cysteine residues (Figure 2). The sulfonate moiety participates in several hydrogen bonding interactions with Asn75, Thr186, and Cys185. The benzene moiety also interacts with Ser11 via an OH–π interaction. These moieties both appear to contribute to the recognition of compound **2**, and thus the optimization strategy focused on the addition of substituents that would produce additional interactions while preserving the original contacts. As observed by their solvent exposure and protein proximity (symbolized by light blue shading or a grey dotted line, respectively, in Figure 2), carbon atoms 4, 5, and 6 within the benzene ring could serve as starting points to build on addi-

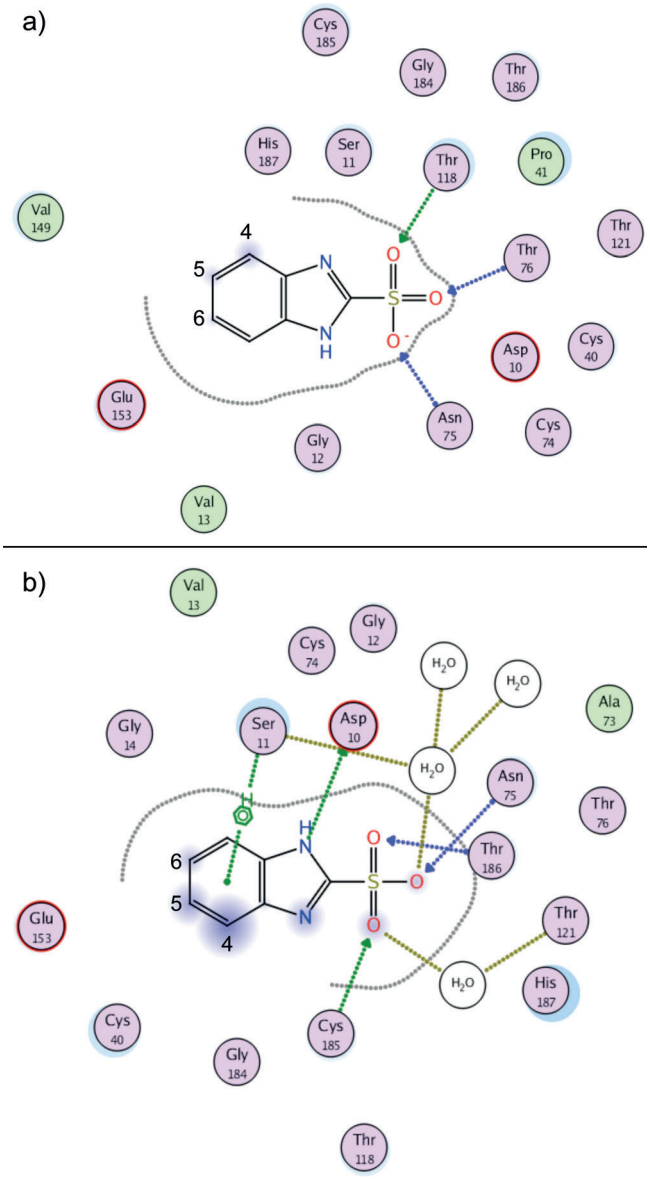

Figure 2. a) Top-ranked binding pose for compound **2** bound to *B. subtilis* GR as predicted by docking. b) Binding pose for compound **2** after 4 ns MD simulation with explicit water.

tional chemical groups without encountering steric clash from active site residues. Depending on their size, substituents added at these positions have the capacity to reach additional binding pockets proximal to the main substrate binding cleft.

Derivative selection and synthesis

An in silico library containing compounds **3**–**35** (Figure 4 below) was developed based on a previously established two-step synthetic process (Scheme 1) and the commercially available 1,2-phenylenediamine derivatives. This synthetic scheme was chosen for its relative ease, while additional chemistry may be attempted in the future to further grow fragments out of the substrate binding cleft. Before any compound was synthesized, the library was subjected to a hybrid ensemble docking scheme, referred to as the flexible enzyme receptor method by steered molecular dynamics (FERM-SMD), previously described by Whalen and co-workers.[12] Figure 3 details how unique conformations of the protein target were generated using steered MD simulations to emulate the substrate unbinding trajectory. Starting with a crystal structure of D-glutamate bound to GR, D-glutamate is pulled from the active site over the course of the simulation. In the process, the enzyme alters its structural conformation to allow substrate passage from the buried binding cleft. Three snapshots were chosen to represent three distinct structural states, distinguished by the entrance to the binding cleft: closed, partially open, and fully open (Figure 3). Compounds were docked to all three structures, and their predicted binding affinities were adjusted according to the respective protein solvation energy (these varied greatly and affected the accuracy of binding affinity calculations) and weighted to indicate relative binding specificity to one of the three receptors. Previous studies have shown that the final score produced by FERM-SMD, deemed FERMscore, shares a high correlation with experimental binding affinities, particularly for congeneric ligands of GR. On a set of 17 ligands, FERM-SMD has a predictive accuracy of ± 1 kcal mol^{-1}.[12]

FERMscores for the library of interest, spanning from 0.4 to 13.7, are indicated in Table 1. The parent compound **2** scored the third-highest FERMscore. The two compounds giving higher calculated FERMscores (compounds **18** and **29**) in addition to a third compound, **4**, which possessed a FERMscore in the top 15% of all derivatives, were synthesized under contract by Enamine Ltd. (see Experimental Section), and all compounds were heretofore synthetically novel. In addition to the compounds predicted to have improved binding affinity, three immediately available compounds (**15**, **24**, and **26**) were acquired to test the predictive capacity of the employed scoring method (Figure 4). Compound **7** had an intermediate FERMscore, but distinct chemotype, which had not been tested on any GR and was therefore chosen for testing. Unfortunately, several attempts to synthesize compound **7** were unsuccessful, and it was eventually abandoned. The experimental results are detailed below.

In vitro testing of derivatives

Inhibition constants (K_i) were acquired for all derivatives against purified GR from *B. subtilis* (Figure 5, Table 2). Compounds **15**, **24**, and **26**, all possessing predicted FERMscores lower than the parent compound, gave K_i values greater than or within error of that of the parent compound. Compound **24**

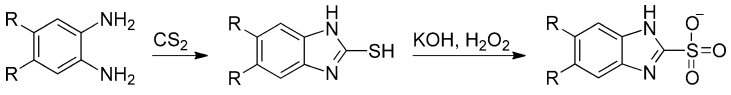

Scheme 1. General scheme for the synthesis of 1*H*-benzimidazole-2-sulfonic acid derivatives from various phenylenediamine starting points.

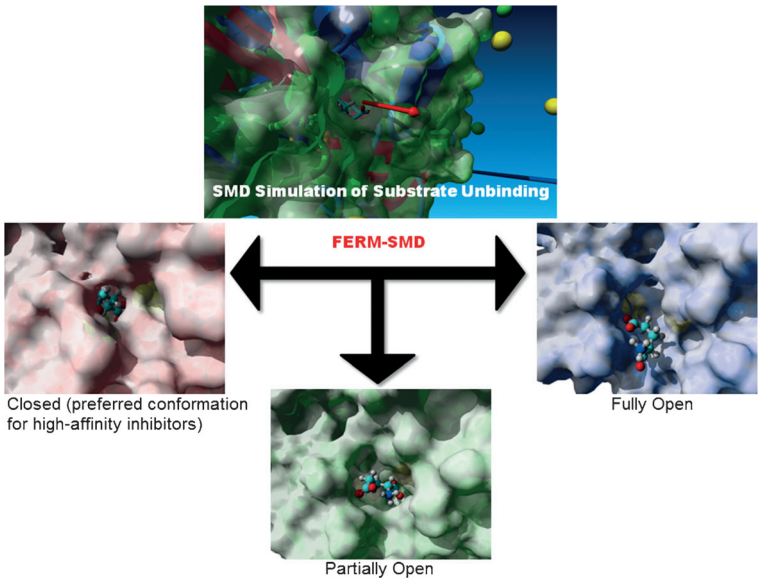

Figure 3. A steered MD simulation was conducted on the glutamate-bound crystal structure of *B. subtilis* GR. A force was applied on the bound substrate along the vector indicated in the top picture (red arrow). Structures were obtained along the unbinding trajectory that correspond approximately to the following states: closed, partially open, and fully open. With substrate removed, these structures then provide the receptors for ensemble docking of the derivative library. Previous results indicate that the highest-affinity inhibitors bind preferentially to the closed conformation over the partially and fully open conformations.

Table 1. FERMscore assignments as predicted by FERM-SMD, ranked from highest to lowest score, corresponding to highest to lowest predicted binding affinity.[a]

Compd	FERMscore	Compd	FERMscore
29	13.7	**26**	1.20
18	9.25	**7**	1.15
2	8.28	**6**	1.10
5	4.92	**23**	1.03
4	4.45	**15**	0.969
34	3.75	**20**	0.902
14	3.23	**33**	0.792
13	2.99	**16**	0.781
12	2.98	**32**	0.756
9	2.97	**28**	0.756
8	2.33	**35**	0.751
22	1.76	**25**	0.750
17	1.64	**3**	0.732
21	1.44	**10**	0.723
11	1.31	**24**	0.643
19	1.29	**31**	0.534
30	1.28	**27**	0.406

[a] Compounds of interest are highlighted accordingly: green = compounds tested with high predicted affinity; cyan = parent scaffold; red = compounds tested with low predicted affinity; yellow = compound synthesis attempted, yet unsuccessful.

suffered from a nearly 100-fold loss in binding affinity, which was well predicted by FERM-SMD, as it possessed the lowest FERMscore of the compounds tested. Of the compounds predicted to be higher-affinity binders by FERMscore, compounds **18** and **29** have K_i values within error of the parent compound, although the K_i value of **29** is improved: 6.4 versus 9 μM. This result was not surprising considering the FERMscores only vary by 5.4 units between the parent scaffold and the highest-scoring derivative. Compound **4** is also predicted to have high affinity, and shows fourfold improved affinity over the parent compound with a K_i value of 2.5 μM. This is the most potent non-glutamate-based competitive inhibitor of GR to date. Overall, FERM-SMD was successful in distinguishing between tight binding derivatives (K_i from 2.5 to 12 μM) and weaker binding derivatives (K_i between 13 and 830 μM).

Ligand and lipophilic efficiencies (LE and LiPE) were calculated for each derivative (Table 2). LE is a way to describe normalized binding affinities for compounds of differing molecular weights.[14] Several studies have also shown that fragment-based drug discovery is more successful if high LE is maintained through lead optimization.[14] This practice lowers the occurrence of so-called "molecular obesity" as compounds are modified to achieve higher potency and favorable pharmacokinetic/pharmacodynamic profiles.[14b] With the exception of compound **15**, each assayed derivative maintained high ligand efficiency (LE > 0.3 kcal mol^{-1} atom^{-1}). Of the compounds predicted to be high affinity by the FERM-SMD method, compounds **4** and **29** exhibited higher efficiency than compound **18** (0.45, 0.34, and 0.30, respectively). Lipophilic efficiency is another measure that is indicative of successful passage down the drug development pipeline, in which affinity values are normalized for the partition coefficient (log *P*) of the inhibitor.[15] Compounds **4** and **29** benefit from an improved LiPE (6.0 and 6.6, respectively) over the parent scaffold (5.3). LE and LiPE values equal to or greater than 0.3 kcal mol^{-1} atom^{-1} and 6.0, respectively, are in the desirable range for further study and optimization.[14a,15]

Table 2. In vitro results for derivatives of the parent scaffold, **2**.

Compd	K_i [μM]	LE [kcal mol^{-1} atom^{-1}][a]	LiPE[b]
2	9.0 ± 2.0	0.53	5.3
4	2.5 ± 0.4	0.45	6.0
15	21 ± 5.0	0.46	4.4
18	12 ± 3.6	0.30	5.0
24	830 ± 75	0.20	1.9
26	13 ± 2.4	0.48	4.5
29	6.4 ± 3.5	0.34	6.6

[a] Ligand efficiencies determined by converting K_i values into binding energies and dividing by the number of non-hydrogen atoms. [b] Lipophilic efficiencies determined by subtracting log *P* values from the log(K_i) for each compound.

Novel compounds were also tested for the formation of colloidal aggregates, a common cause of false-positive results. Previous studies have revealed that GR is susceptible to inhibi-

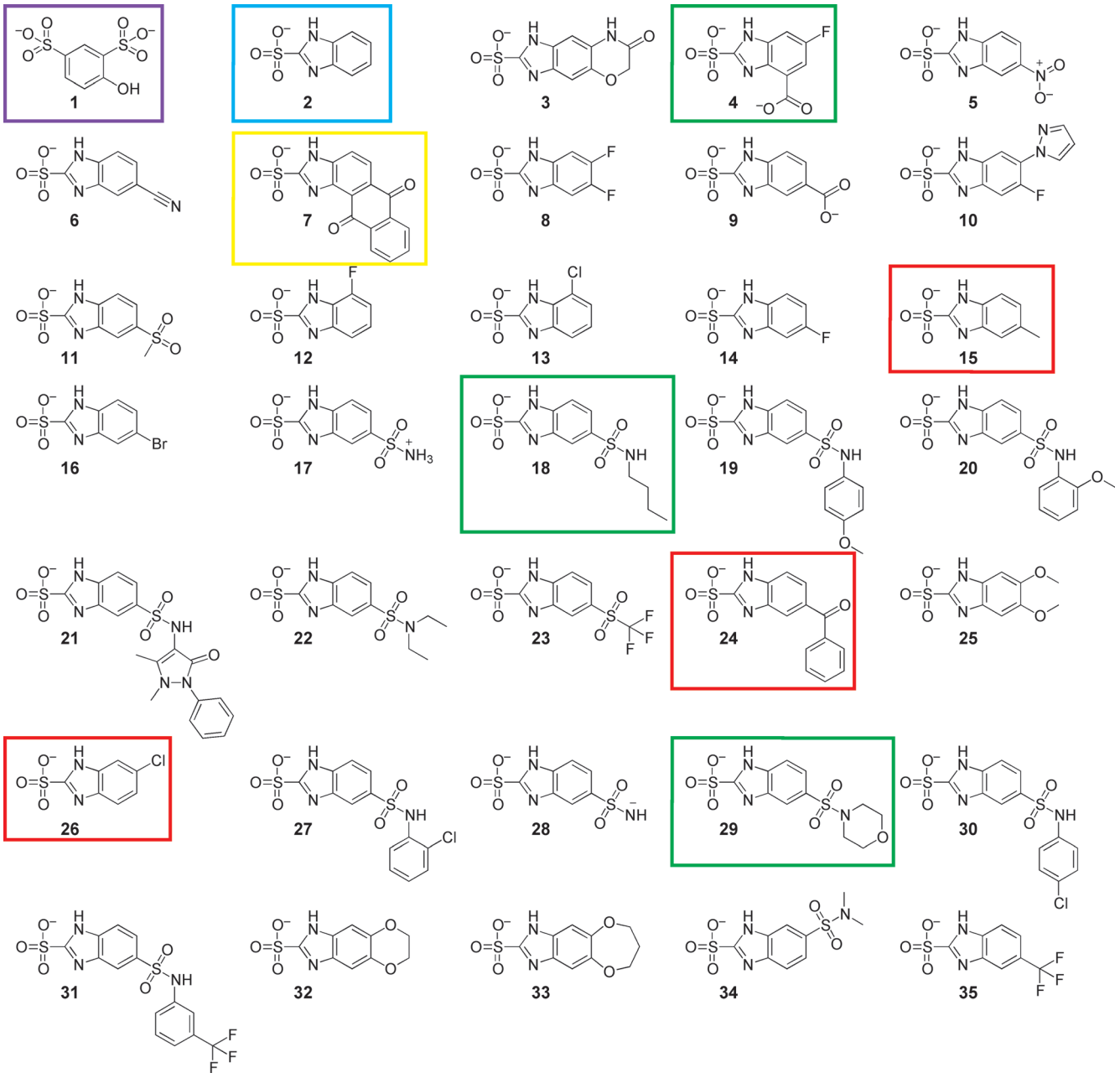

Figure 4. Parent scaffolds and lead derivatives considered in this study. Compounds of interest are highlighted accordingly: lavender = original virtual screening hit; cyan = parent scaffold; green = compounds tested with high predicted affinity; red = compounds tested with low predicted affinity; yellow = compound synthesis attempted, yet unsuccessful.

tion by colloidal aggregates in a non-drug-like fashion. To distinguish between inhibition via colloidal aggregation and true binding, enzyme activity was measured in the presence of the inhibitor in question, as well as a sub-micellular concentration of detergent, 0.01% Triton X-100. In the event that a given compound inhibits an enzyme by colloidal aggregation, the apparent inhibition will be completely relieved in the presence of detergent. Colloidal aggregates must be abandoned due to their non-drug-like mechanism. All novel compounds tested in this study proved not to operate through a colloidal aggregate mechanism (Supporting Information figure S10).

In vivo testing of biological activity

To assess the capacity of these compounds to reach the enzyme target in vivo, inhibition of bacterial growth as well as capacity to induce cell lysis was assayed with several species of bacteria. *B. subtilis* was investigated, as the isozyme of GR from this species was the model for all in silico predictions. Additionally, *E. coli* and *S. aureus* were investigated, as each provides a unique challenge for inhibitor compounds: an additional physical barrier to entry in the case of Gram-negative *E. coli*, and an abundance of efflux pumps in the case of *S. aureus*.[16]

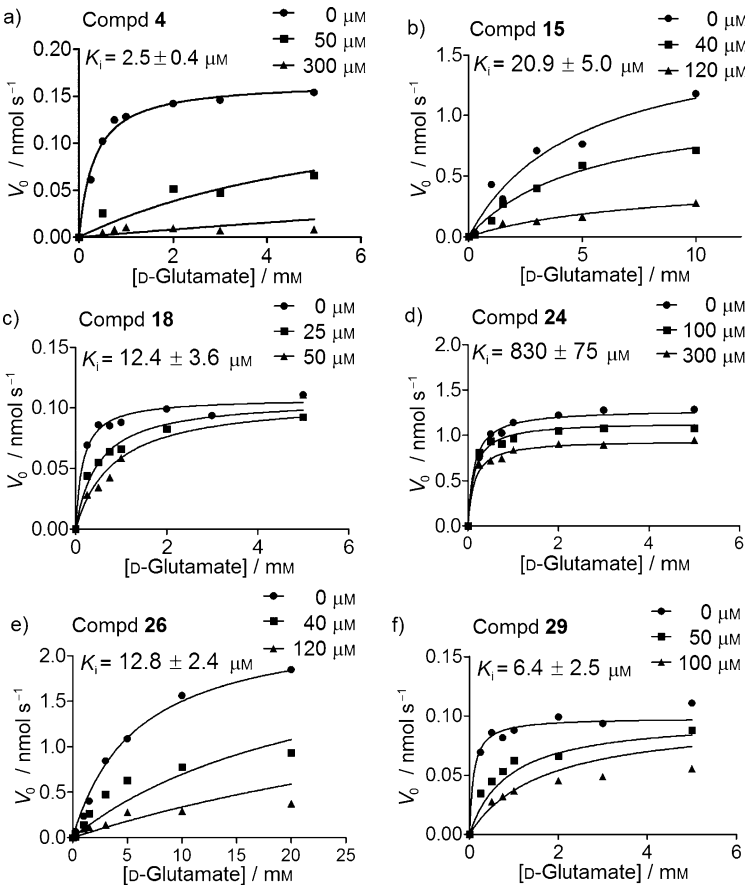

Figure 5. In vitro inhibition data used to acquire K_i values for each derivative.

highly specific for *B. subtilis*, showing no significant growth inhibition at concentrations <3 mg mL^{-1} for *E. coli* and *S. aureus* (Table 3). In contrast, compound **4** shows growth inhibition of both *E. coli* and *S. aureus* at concentrations approximately twofold higher than the MIC_{50} value against *B. subtilis* (Table 3). Examination of their respective chemical structures yields one possible rationale for this distinction (see Figure 4 for structures). Compound **4** possesses a more compact structure, most likely making contacts specific to the most buried and most highly conserved region of the GR active site. Compounds **18** and **29** contain bulkier chemical additions to the benzene ring that may clash with the outer region of the GR active site, which is a more structurally diverse region. These in vitro (and in silico) results support the fragment-based strategy of growing the scaffold out of the highly buried active site without sacrificing the original contacts.

To determine the mechanism of action of the derivatives in this study, a commercially available cytotoxicity assay, CytoTox-Glo (Promega), marketed for use with mammalian cells, was adapted for use with the examined bacterial species. The relationship between cytotoxicity—specifically cell lysis—and the readout (luminescence) is outlined in Figure 8. If the compounds reach the GR target and inhibit the production of D-glutamate, the lack of this key component results in an overall breakdown in peptidoglycan synthesis, and subsequent cell lysis caused by osmotic stress. Lysed cells then leak intracellular proteases into the surrounding media. The CytoTox-Glo reagent is composed of a pro-luciferin substrate, which once cleaved by proteases, can be acted upon by a supplied luciferase to produce the luminescent readout. Controls using USFDA-approved antibiotics with known mechanisms of action were conducted to optimize the provided reagents (Figure 9a). *S. aureus* was exposed to varying concentrations of ampicillin (a transpeptidase inhibitor) or tetracycline (a microbial ribosome inhibitor) for 24 h, and then incubated with the CytoTox-Glo reagent. As expected, ampicillin yields a dose-dependent increase in luminescence, while tetracycline elicits no increase in luminescence at concentrations up to 100-fold the published MIC_{50} value (Fig-

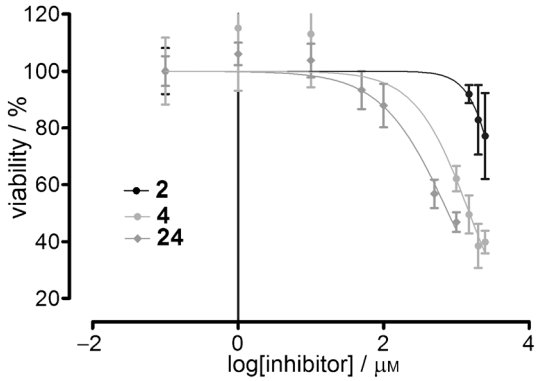

Figure 6. MIC_{50} curves for the parent scaffold and the two most potent derivatives against *B. subtilis*.

Table 3. MIC_{50} values for tested derivatives.

Compd	MIC_{50} [mg mL^{-1}]		
	B. subtilis	*E. coli*	*S. aureus*
2	0.72 ± 0.06	–	–
4	0.26 ± 0.11	1.6 ± 0.20	1.0 ± 0.25
15	>3	–	–
18	0.36 ± 0.02	>3	>3
24	0.14 ± 0.02	–	–
26	>3	–	–
29	0.32 ± 0.01	>3	>3

All tested derivatives of compound **2** show increased potency with regards to growth inhibition of *B. subtilis* (Figure 6). MIC_{50} values were increased two- to threefold over the parent scaffold (Table 3). Surprisingly, the least potent compound in vitro, **24**, shows the greatest potency in vivo. This result suggests that factors other than enzyme binding affinity may complicate the overall efficacy of this chemotype of antimicrobial compounds.

Compounds **4**, **18**, and **29** were also tested against *E. coli* and *S. aureus* (Figure 7). Compounds **18** and **29** were both

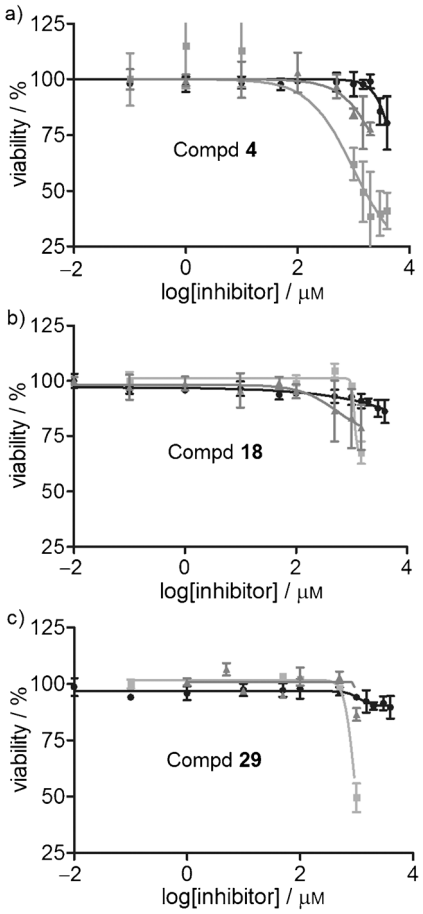

Figure 7. MIC_{50} curves for highest-ranked derivatives, by FERMscore, comparing species specificity between *E. coli* (●), *B. subtilis* (■), and *S. aureus* (▲).

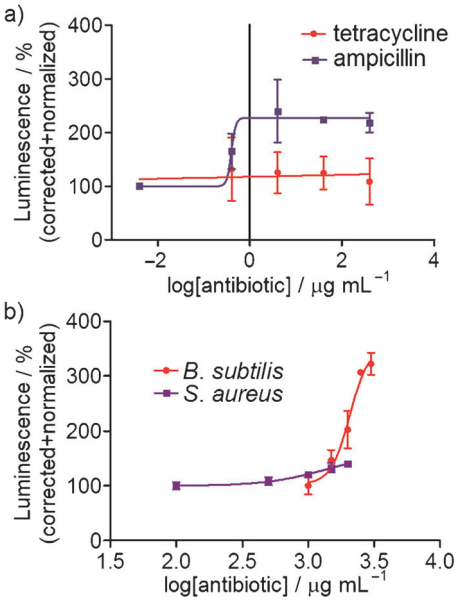

Figure 9. Controls for a commercially available cytotoxicity assay that monitors cell wall lysis with a luminescent readout. a) Bacteria treated with two antibiotics, only one using a mechanism of action that interferes with peptidoglycan synthesis, shows distinct luminescent dose responses. b) Cell lysis data for *S. aureus* and *B. subtilis* cultures treated for 24 h with compound **4**. Luminescence is measured in arbitrary units, corrected for the cell density of the sample (variable depending on growth inhibition), and is presented as a percentage of untreated cell luminescence.

ure 9a). This optimized assay was then applied to cells treated with our inhibitor derivatives.

The modified CytoTox-Glo assay confirmed **4** as acting via an inhibitory mechanism that affects the peptidoglycan with both *S. aureus* and *B. subtilis* (Figure 9b). Luminescence increases concurrently with increased dosing of compound **4** for *S. aureus*. Although the assayed concentrations do not span the entire MIC_{50} range owing to solubility limitations, an approximate 40% increase in luminescence was observed in the millimolar inhibitor concentration range. For *B. subtilis*, the species for which compound **4** elicits greater growth inhibition, we observed a dose-dependent increase of 400% in luminescence in the low-millimolar range. The observed EC_{50} for lysis occurs at 520 μg mL^{-1}, a concentration only slightly above that of the MIC_{50} value for growth inhibition (260 μg mL^{-1}). The proximity of these two values supports cell lysis as the main cause of cell death. Considering the many barriers an antibacterial compound must overcome—both physical (peptidoglycan and efflux) and chemical (metabolism)—in order to reach the desired target protein, the ability of compound **4** to cause cell lysis is excellent support for its further development as an antibacterial therapeutic.

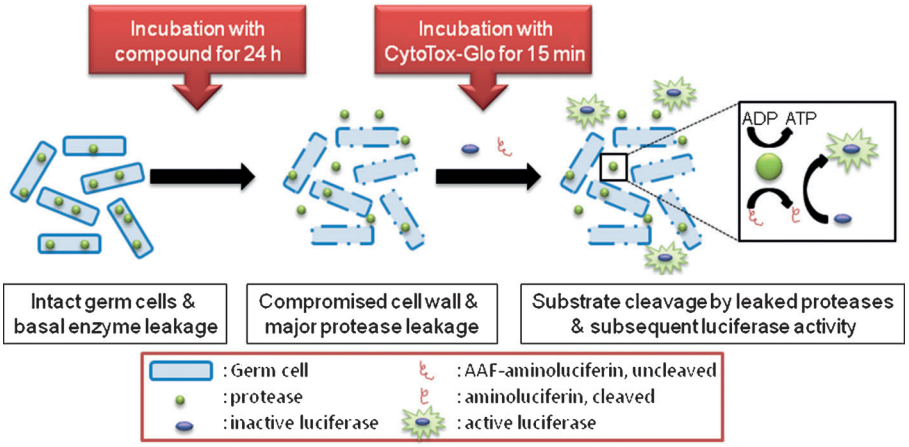

Figure 8. Illustration of the treatment of bacterial cells in the CytoTox-Glo assay. The CytoTox-Glo reagent contains both the protease substrate, AAF–luciferin, as well as luciferase. Bacterial cells contain intracellular enzymes capable of cleaving AAF–luciferin, releasing luciferin, the substrate of luciferase.

Conclusions

This study summarizes the successful use of a novel in silico docking and scoring scheme for

the selection of derivatives of a lead scaffold via rank-ordering of binding affinity. The model system used herein uses the antibacterial target, glutamate racemase, and a low-micromolar competitive inhibitor, 1*H*-benzimidazole-2-sulfonic acid (compound **2**), as the lead compound. This platform could be used for optimization of lead compounds for other flexible drug targets. In current lead optimization campaigns, the rate-limiting step is often the acquisition of high-resolution structural data, particularly for flexible enzymes, on the enzyme–drug complex. Binding pose predictions made by docking software have been largely validated as correct in many cases by comparison with experimental data; specifically, several programs place ligands within 2 Å RMSD of the crystallographically determined pose for over 90% of assessed ligands.[17] The perennial problem lies in the ability of the scoring functions to accurately rank-order docked ligands across a variety of targets.[17] By developing an in silico method of derivative ranking based on the docked complex of the parent scaffold with a predictive error of only ± 1 kcal mol^{-1} for binding energy, we can remove the need for time- and resource-consuming NMR or X-ray crystallography experiments. Additionally, the ability to predict the binding potency of potential derivatives renders the chemical synthesis of weak binders unnecessary. Herein we show that the described scheme guides optimization of a lead compound with minimal investment of resources and time.

The goal of this exercise was to modify the existing chemical scaffold in order to increase binding affinity to the target enzyme, while also maintaining favorable physicochemical properties (here, ligand efficiency and lipophilic efficiency) and biological activity. A docked complex of compound **2** and GR was used to assess the optimal locations for substituent addition. Based on that analysis, a library of 33 derivatives of compound **2** were subjected to a hybrid ensemble docking scheme, FERM-SMD, in order to rank their potential binding potencies. Of the 33 derivatives, six compounds were tested experimentally, producing the final selection of compound **4**. Compound **4** has increased binding affinity for the purified enzyme: 2.5 versus 9 μM, high LE: 0.45 kcal mol^{-1} atom^{-1}, high LiPE: 6.0, increased growth inhibition of *B. subtilis*: $MIC_{50} = 260$ versus 720 μg mL^{-1}, and finally, effective bacterial cell lysis: $EC_{50,lysis} = 520$ μg mL^{-1}. The FERM-SMD methodology has afforded a facile optimization from a high-LE hit with relatively low synthetic cost by precisely identifying a binding rank-order. Future studies will focus these techniques on increasingly more complex derivative libraries to achieve even greater in vitro and biological activity.

Experimental Section

Docking and FERM-SMD: virtual screening

The original FERM-SMD method is described in great detail by Whalen and co-workers.[12] BISA derivatives were prepared in silico using MOE v2011.10[18] (Chemical Computing Group). An ensemble of GR structures was generated using steered molecular dynamics simulation. Three structures were chosen at approximately the most closed (corresponding to 0 ps simulation time), partially open (13.9 ps simulation time), and fully open (20 ps simulation time). Docking to the ensemble of GR structures was achieved with YASARA v9.11.9,[19] which uses an optimized version of AutoDock 4.[20] Simulation cells were centered around the active site and expanded to include the residues surrounding the cleft entrance. Simulation cells had the following dimensions (in Å): "0 ps" receptor = 18.75 × 20.19 × 19.29; "13.9 ps" receptor = 19.08 × 21.56 × 18.07; and "20 ps" receptor = 18.94 × 21.31 × 18.93. Receptor–ligand docking combinations that resulted in more than one high-ranking pose were visually assessed by the authors, and the pose that placed the core scaffold in a position most similar to the parent scaffold position was chosen as the "true" pose. Resulting binding energies and affinities for docking to all three receptors were then imported into Excel (Microsoft Office) and adjusted for receptor-protein solvation, producing a final FERMscore.[12]

Compound synthesis and acquisition

Compound **1** (cat.# BAS 00124393, >98% purity) was acquired from Asinex Ltd. (Moscow, Russia). Compound **2** (cat.# 530646, 98% purity) was acquired from Sigma–Aldrich (St. Louis, MO, USA). Compound **15** (cat.# 5648649, 100% purity) was acquired from ChemBridge Corp. (San Diego, CA, USA). Compound **24** (cat.# STK695918, 98% purity) was acquired from Vitas-M Laboratories Ltd. (Moscow, Russia). Compound **26** (cat.# Z57080960, 95% purity) was acquired from Enamine Ltd. (Kiev, Ukraine). Compounds **4**, **18**, and **29** were synthesized according to published procedures by collaborators at Enamine Ltd. (Kiev, Ukraine) following the synthetic process outlined in Scheme 1.[21] ^{1}H NMR spectra for each synthesized compound are provided in the Supporting Information (figures S3–S5). HPLC data showing purity analysis are also available in the Supporting Information for each newly synthesized compound (figures S6–S8)

Protein expression and purification

Genes of glutamate racemase were isolated from *B. subtilis*, *B. anthra*cis (two isozymes), and *F. tularensis*, and expressed in *E. coli* and purified by using a protocol previously described by Whalen and co-workers.[12] Briefly, His_6-tagged recombinant proteins were purified by a two-step process composed of cobalt-affinity (His-Select Affinity Resin, Sigma–Aldrich) and anion-exchange (UNO Q Continuous Bed column, BioRad) chromatography. Proteins were stored in buffer containing 100 mM NaCl, 50 mM Tris, 0.2 mM DTT, pH 8.0 at a concentration of 7–10 mg mL^{-1}. Molecular weight was confirmed by SDS-PAGE analysis (Supporting Information figure S1), and degree of protein folding was assessed by circular dichroism (CD; Supporting Information figure S2).

In vitro inhibition of enzyme activity

Steady-state kinetics for D-to-L racemization was measured by CD on a JASCO J-715 spectropolarimeter. All compound stocks were made up in 50 mM potassium borate buffer, pH 8.0, at concentrations in the range of 25–100 mM depending on compound solubility. Reactions were carried out at 25 °C in 50 mM potassium borate buffer, pH 8.0, with 1 μM purified enzyme. CD signal (mdeg) was measured continuously at 220 nm for 10 min. Plots of CD versus time were fit linearly to obtain initial velocity. Substrate was varied from 0.25 to 5 mM. For K_i determination, three Michaelis–Menten curves were obtained for each inhibitor: one in the absence of inhibitor, and two in varying concentrations of inhibitor. A single data set, composed of three curves, was fit to a competitive inhibi-

tion model using GraphPad Prism v.5.0,[22] and the K_i was obtained as a best-fit value. For IC_{50} determination, reactions were supplemented with varying concentrations of inhibitor, and the observed V_0 (nmol s^{-1}) was normalized to a percent activity value based on an uninhibited reaction. Percent activity values were plotted versus the log of the inhibitor concentration. The data set was then fit to a log[inhibitor] versus response model (with variable slope) to calculate the IC_{50}, using GraphPad Prism v.5.0.[22] For LiPE calculations, compound log *P* values for the ionic species were calculated with MarvinSketch (ChemAxon).

In vivo inhibition of bacterial growth

A 5 mL culture of bacteria (*B. subtilis* DB104, *E. coli* Acella, or *S. aureus* ATCC 12600) was incubated overnight at 37 °C in tryptic soy broth one day prior to assay; 96-well plates were prepared with 2× media, phosphate-buffered saline, the compound of interest, and a 20 μL inoculum of bacteria, totaling 200 μL per well. Compound stocks were prepared in phosphate-buffered saline at a concentration of 10, 12.5, or 25 mM, depending on compound solubility. A serial dilution ranging from 0.1 to 3000 μM for the compound of interest was assayed. The overnight culture, at an optical density of ~2.0, was diluted 20-fold in water prior to inoculation, such that initial optical densities were ~0.01. A table of reagent volumes and diagram of plate layout can be found in figure S9 of the Supporting Information. Plates were mixed and incubated at 37 °C for 24 h. Absorbance at λ 600 nm was measured on a GloMax-Multi Detection System. MIC_{50} values were determined by fitting data to a log[inhibitor] versus response model using GraphPad Prism v.5.0.[22] The bottom and top values are constrained to 20 and 100%, respectively.

Cell wall lysis assay

Bacterial cell wall lysis was assayed using a modification of the CytoTox-Glo assay[23] (Promega): 100 μL of the contents of a 96-well plate treated as described above were moved to a white, round-bottom, 96-well plate. CytoTox-Glo reagent buffer (25 μL) was added to each well, mixed and incubated at room temperature in the dark for 15 min. Luminescence was measured on a GloMax-Multi Detection System. Luminescent values were normalized based on the absorbance value at λ 600 nm for each respective well. Data was then fit to a log[agonist] versus response model, with no upper or lower constraints, using GraphPad Prism v5.0.[22]

Acknowledgements

This work was supported by the US National Institutes of Health (NIH) grant numbers R01 GM097373 (M.A.S.) as well as the Chemical Biology Training Grant at UIUC (K.L.W.). Special thanks go to Irina Yavnyuk and Tatiana Galushka for facilitating our fruitful collaboration with Enamine Ltd.

Keywords: antibiotics · fragment-based drug discovery · glutamate racemase · heterocyclic aromatics · inhibitors

[1] D. J. Payne, M. N. Gwynn, D. J. Holmes, D. L. Pompliano, *Nat. Rev. Drug Discovery* **2007**, *6*, 29 – 40.
[2] R. O'Shea, H. E. Moser, *J. Med. Chem.* **2008**, *51*, 2871 – 2878.
[3] J. W.-H. Li, J. C. Vederas, *Science* **2009**, *325*, 161 – 165.
[4] T. D. Bugg, C. T. Walsh, *Nat. Prod. Rep.* **1992**, *9*, 199 – 215.
[5] a) A. E. Belanger, J. C. Porter, G. F. Hatfull, *J. Bacteriol.* **2000**, *182*, 6854 – 6856; b) M. R. de Roubin, D. Mengin-Lecreulx, J. van Heijenoort, *J. Gen. Microbiol.* **1992**, *138*, 1751 – 1757; c) B. H. Hebeler, F. E. Young, *J. Bacteriol.* **1975**, *122*, 385 – 392.
[6] T. Lundqvist, S. L. Fisher, G. Kern, R. H. Folmer, Y. Xue, D. T. Newton, T. A. Keating, R. A. Alm, B. L. de Jonge, *Nature* **2007**, *447*, 817 – 822.
[7] P. Conti, L. Tamborini, A. Pinto, A. Blondel, P. Minoprio, A. Mozzarelli, C. De Micheli, *Chem. Rev.* **2011**, *111*, 6919 – 6946.
[8] a) E. D. LoVullo, C. R. Molins-Schneekloth, H. P. Schweizer, M. S. Pavelka, Jr., *Microbiology* **2009**, *155*, 1152 – 1163; b) K. Y. Shatalin, A. A. Neyfakh, *FEMS Microbiol. Lett.* **2005**, *245*, 315 – 319.
[9] a) A. de Dios, L. Prieto, J. A. Martin, A. Rubio, J. Ezquerra, M. Tebbe, B. L. de Uralde, J. Martin, A. Sanchez, D. L. LeTourneau, J. E. McGee, C. Boylan, T. R. Parr, Jr., M. C. Smith, *J. Med. Chem.* **2002**, *45*, 4559 – 4570; b) M. May, S. Mehboob, D. C. Mulhearn, Z. Wang, H. Yu, G. R. Thatcher, B. D. Santarsiero, M. E. Johnson, A. D. Mesecar, *J. Mol. Biol.* **2007**, *371*, 1219 – 1237.
[10] K. L. Whalen, K. L. Pankow, S. R. Blanke, M. A. Spies, *ACS Med. Chem. Lett.* **2010**, *8*, 9 – 13.
[11] M. A. Spies, J. G. Reese, D. Dodd, K. L. Pankow, S. R. Blanke, J. Baudry, *J. Am. Chem. Soc.* **2009**, *131*, 5274 – 5284.
[12] K. L. Whalen, K. M. Chang, M. A. Spies, *Mol. Inf.* **2011**, *30*, 459 – 471.
[13] C. W. Murray, D. C. Rees, *Nat. Chem.* **2009**, *1*, 187 – 192.
[14] a) A. L. Hopkins, C. R. Groom, A. Alex, *Drug Discovery Today* **2004**, *9*, 430 – 431; b) M. Hann, *Med. Chem. Commun.* **2011**, *2*, 349 – 355.
[15] P. D. Leeson, B. Springthorpe, *Nat. Rev. Drug Discovery* **2007**, *6*, 881 – 890.
[16] M. Kuroda, T. Ohta, I. Uchiyama, T. Baba, H. Yuzawa, I. Kobayashi, L. Cui, A. Oguchi, K. Aoki, Y. Nagai, J. Lian, T. Ito, M. Kanamori, H. Matsumaru, A. Maruyama, H. Murakami, A. Hosoyama, Y. Mizutani-Ui, N. K. Takahashi, T. Sawano, R. Inoue, C. Kaito, K. Sekimizu, H. Hirakawa, S. Kuhara, S. Goto, J. Yabuzaki, M. Kanehisa, A. Yamashita, K. Oshima, K. Furuya, C. Yoshino, T. Shiba, M. Hattori, N. Ogasawara, H. Hayashi, K. Hiramatsu, *Lancet* **2001**, *357*, 1225 – 1240.
[17] G. L. Warren, C. E. Peishoff, M. S. Head, *Computational and Structural Approaches to Drug Discovery: Ligand – Protein Interactions, Vol. 1, 1st ed.*, RSC, Cambridge, **2008**.
[18] Molecular Operating Environment (MOE) v2011.10, **2011**, Chemical Computing Group Inc., 1010 Sherbooke Street West, Suite 910, Montreal, QC, H3A 2R7 (Canada).
[19] a) E. Krieger, YASARA v9.11.9, **2011**, YASARA Biosciences GmbH, Vienna (Austria); b) E. Krieger, G. Koraimann, G. Vriend, *Proteins* **2002**, *47*, 393 – 402.
[20] G. M. Morris, R. Huey, W. Lindstrom, M. F. Sanner, R. K. Belew, D. S. Goodsell, A. J. Olson, *J. Comput. Chem.* **2009**, *30*, 2785 – 2791.
[21] A. Mavorova, P. Denkova, Y. A. Tsenov, K. K. Anichina, D. I. Vutchev, *Bioorg. Med. Chem.* **2007**, *15*, 6291 – 6297.
[22] GraphPad Prism v5.0, **2007**, GraphPad Software, San Diego, CA (USA).
[23] A. L. Niles, R. A. Moravec, P. E. Hesselberth, M. A. Scurria, W. J. Daily, T. L. Riss, *Anal. Biochem.* **2007**, *366*, 197 – 206.

Received: June 15, 2013
Published online on ■■ ■■, 0000